

Modeling deformation behavior of Cu–Zr–Al bulk metallic glass matrix composites

S. Pauly^{*}, G. Liu, G. Wang, J. Das, K. B. Kim, U. Kühn, D. H. Kim, and J. Eckert

Citation: *Appl. Phys. Lett.* **95**, 101906 (2009); doi: 10.1063/1.3222973

View online: <http://dx.doi.org/10.1063/1.3222973>

View Table of Contents: <http://aip.scitation.org/toc/apl/95/10>

Published by the American Institute of Physics

Articles you may be interested in

[Plasticity-improved Zr–Cu–Al bulk metallic glass matrix composites containing martensite phase](#)

Applied Physics Letters **87**, 051905 (2005); 10.1063/1.2006218

[Bulk metallic glass matrix composites](#)

Applied Physics Letters **71**, 3808 (1998); 10.1063/1.120512

[ZrNbCuNiAl bulk metallic glass matrix composites containing dendritic bcc phase precipitates](#)

Applied Physics Letters **80**, 2478 (2002); 10.1063/1.1467707

[Correlation between the microstructures and the deformation mechanisms of CuZr-based bulk metallic glass composites](#)

AIP Advances **3**, 012116 (2013); 10.1063/1.4789516

[Pronounced ductility in CuZrAl ternary bulk metallic glass composites with optimized microstructure through melt adjustment](#)

AIP Advances **2**, 032176 (2012); 10.1063/1.4754853

[Heterogeneity of a \$\text{Cu}_{47.5}\text{Zr}_{47.5}\text{Al}_5\$ bulk metallic glass](#)

Applied Physics Letters **88**, 051911 (2006); 10.1063/1.2171472



**THE WORLD'S RESOURCE FOR
VARIABLE TEMPERATURE
SOLID STATE CHARACTERIZATION**



OPTICAL STUDIES SYSTEMS



SEEBECK STUDIES SYSTEMS



MICROPROBE STATIONS



HALL EFFECT STUDY SYSTEMS AND MAGNETS



WWW.MMR-TECH.COM

Modeling deformation behavior of Cu–Zr–Al bulk metallic glass matrix composites

S. Pauly,^{1,a)} G. Liu,² G. Wang,¹ J. Das,³ K. B. Kim,⁴ U. Kühn,¹ D. H. Kim,⁵ and J. Eckert^{1,6}

¹IFW Dresden, Institut für Komplexe Materialien, Helmholtzstraße 20 D-01069 Dresden, Germany

²State Key Laboratory for Mechanical Behavior of Materials, School of Materials Science and Engineering, Xi'an Jiaotong University, Xi'an, 710049, People's Republic of China

³Department of Metallurgical and Materials Engineering, Indian Institute of Technology, Kharagpur-721 302, West Bengal, India

⁴Department of Advanced Materials Engineering, Sejong University, 98 Gunja-dong, Gwangjin-gu, Seoul 143-747, Republic of Korea

⁵Department of Metallurgical Engineering, Center for Non-crystalline Materials, Yonsei University, Seoul 120-749, Republic of Korea

⁶TU Dresden, Institut für Werkstoffwissenschaft, D-01062 Dresden, Germany

(Received 4 July 2009; accepted 16 August 2009; published online 9 September 2009)

In the present work we prepared an *in situ* Cu_{47.5}Zr_{47.5}Al₅ bulk metallic glass matrix composite derived from the shape memory alloy CuZr. We use a strength model, which considers percolation and a three-microstructural-element body approach, to understand the effect of the crystalline phase on the yield stress and the fracture strain under compressive loading, respectively. The intrinsic work-hardenability due to the martensitic transformation of the crystalline phase causes significant work hardening also of the composite material. © 2009 American Institute of Physics.

[doi:10.1063/1.3222973]

Plastic strain in bulk metallic glasses (BMGs) is highly localized in shear bands with a thickness of only a few nanometers, which severely limits the plastic deformability.¹ There are different approaches how to introduce a somewhat more homogeneous plastic strain in glassy materials among them the synthesis of BMG matrix composites.² However, the increase in plasticity does not necessarily go along with work hardening, another necessity from an engineering point of view.^{3,4}

Among the diversity of BMGs,⁵ CuZr-based alloys are peculiar under two aspects: first, their melts have a relatively strong tendency to vitrify. Even binary and ternary glassy alloys can be obtained in the Cu–Zr system.⁶ Second, crystalline B2 CuZr (*Pm-3m*) shows the shape memory effect.⁷ The cubic primitive B2 structure can undergo a reversible transformation to a monoclinic B19' (*Cm* and *P2₁/m*) structure.⁸ The transformation from B2 CuZr to B19' CuZr is equal to the process in the well-studied shape memory alloy NiTi.⁹ Both peculiarities can be made use of by synthesizing BMG matrix composites in CuZr-based alloy systems, e.g., Cu_{47.5}Zr_{47.5}Al₅. The B2 CuZr phase crystallizes first upon cooling the melt. Even though the B2 CuZr phase is thermodynamically stable only at temperatures above 988 K fast cooling as achieved by Cu-mold casting can prevent the eutectoid decomposition into the low temperature equilibrium phases Cu₁₀Zr₇ and CuZr₂.¹⁰ Proper adjustment of composition and cooling rate suppresses the martensitic transformation and “austenitic” B2 CuZr can be retained at room temperature.¹¹

The BMG matrix composites produced in this work contain different crystalline volume fractions. The crystal size typically ranges from some tens to hundreds of micrometers. We investigated the mechanical properties under uniaxial,

quasistatic compressive loading with the focus on the effect of the second phase on the response of the composite material. The experimental yields strengths were compared with calculations using a strength model, which considers percolation.^{12,13} Furthermore, the fracture strains were calculated by an empirical approach developed by Fan and Miodownik.¹⁴ Despite its importance for understanding the mechanisms in CuZr-based BMG matrix composites, there are no data available in literature on the mechanical properties of B2 CuZr. This gap is filled with the results presented here. Its intrinsic work-hardenability has strong implications on the deformation behavior of the composites.

Cu_{47.5}Zr_{47.5}Al₅ prealloys were synthesized by arc melting the constituting elements (purity of 99.99% or higher). Rods with a diameter of 2 mm were produced via suction casting. The temperature of the Cu_{47.5}Zr_{47.5}Al₅ melt was varied by applying different melting currents. One rod was annealed for 16 h at 1073 K in Ar atmosphere and then quenched to room temperature in an Ar flow within approximately 2 min. The rod was consecutively thermally cycled in a Netzsch DIL 402C dilatometer between 193 and 673 K at a heating rate of 5 K/min to stabilize B2 CuZr at room temperature. The samples were analyzed by means of a Zeiss Axiophot optical microscope and by high-energy x-ray diffraction ($\lambda=0.012\,398\,4$ nm) at BW5 of HASYLAB in Hamburg, Germany. The elastic constants were determined with an Olympus Panametrics-NDT 5900PR ultrasonic testing device. Compression tests were performed on rods with an aspect ratio of two using an Instron 5869 with a constant strain rate of 1×10^{-4} s⁻¹. A laser-extensometer (Fiedler) monitored the strain directly at the sample.

Figure 1 shows the true stress-strain curves of selected Cu_{47.5}Zr_{47.5}Al₅ specimens with different crystalline volume fractions. The inset to Fig. 1 shows three typical microstructures of the composites with different crystalline volume

^{a)}Electronic mail: s.pauly@ifw-dresden.de.

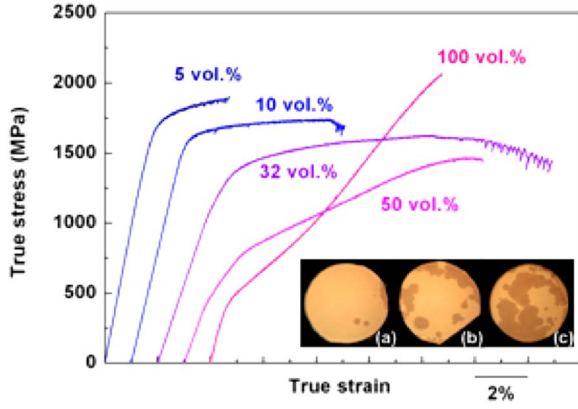


FIG. 1. (Color online) True stress-strain curves of $\text{Cu}_{47.5}\text{Zr}_{47.5}\text{Al}_5$ BMG matrix composites with different crystalline volume fractions. The inset shows the microstructures of rods with a diameter of 2 mm and crystalline volume fractions of (a) 5 vol. %, (b) 30 vol. %, and (c) 50 vol. %.

fractions. The larger the amount of the crystalline phase in the composites (i) the lower the yield stress, (ii) the larger the plasticity, and (iii) the more pronounced the work hardening. This behavior becomes obvious when the fracture strain [Fig. 2(b)] and the yield stress [Fig. 2(a)] are plotted as a function of the crystalline volume fraction. At crystalline volume fractions up to 10 vol. % the yield strength scatters around 1600 MPa and quickly decreases to 1200 MPa when 30 vol. % consist of crystals. In this regime the BMG matrix composite can be described by the rule of mixtures since the matrix has a yield strength much larger than that of the second phase. Yielding of the composite is therefore controlled by yielding of the relatively harder glassy $\text{Cu}_{47.5}\text{Zr}_{47.5}\text{Al}_5$ phase:

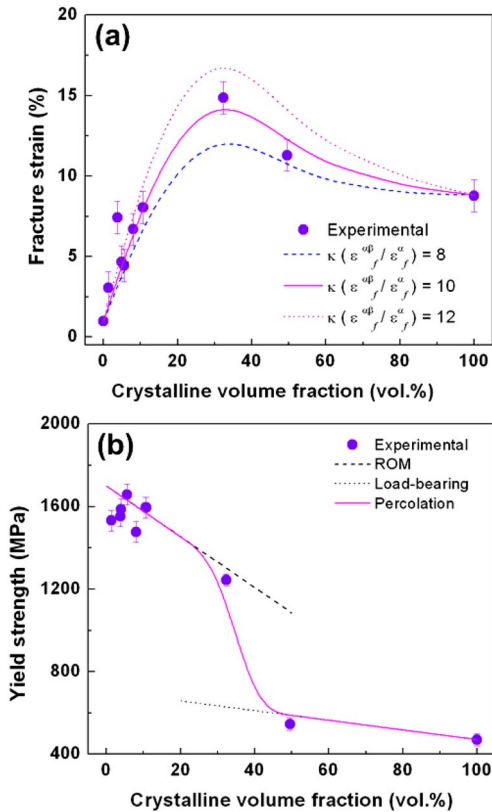


FIG. 2. (Color online) (a) Experimental and calculated values for the fracture strain as a function of the crystalline volume fraction and (b) yield strength vs crystalline volume fraction of the $\text{Cu}_{47.5}\text{Zr}_{47.5}\text{Al}_5$ BMG matrix composites.

TABLE I. Elastic properties of B2 CuZr and the glassy phase in $\text{Cu}_{47.5}\text{Zr}_{47.5}\text{Al}_5$.

Phase	E (GPa)	ν	G (GPa)	B (GPa)
B2 CuZr	82 ± 2	0.385 ± 0.004	29 ± 1	118 ± 3
Glass	89 ± 2	0.373 ± 0.003	33 ± 2	117 ± 3

$$\sigma^c = f_\alpha \sigma^\alpha + f_\beta \sigma^\beta, \quad (1)$$

where f and σ are the volume fraction and the yield strength of the constituent phases, and subscript/superscript α and β refer to B2 CuZr and the BMG, respectively.

At crystalline volume fractions exceeding 50 vol. % the composite can be modeled as a crystalline matrix reinforced with glassy $\text{Cu}_{47.5}\text{Zr}_{47.5}\text{Al}_5$. In this case, the load-bearing model captures the yield stress:¹²

$$\sigma^c = \sigma^\alpha (1 + 0.5 f_\beta). \quad (2)$$

Between those two limiting cases there is a transition determined by a critical crystalline volume fraction (v_{crit}), which has a physical meaning similar to the percolation threshold used to quantify the formation of long-range connectivity in random systems.¹³ In the present case, v_{crit} lies between 30 and 50 vol. %. At the critical volume fraction the crystals interconnect and form a structural framework. This can be readily seen in the micrographs of the rods (inset to Fig. 1). The transition in the microstructure leads to transition in the deformation behavior. The applied strength model [solid line in Fig. 2(b)] describes the experimental data points with satisfying accuracy. The fracture strain versus crystalline volume fraction is displayed in Fig. 2(a). We adapt the empirical approach developed by Fan and Miodownik.¹⁴ The composite is topologically transformed into a three-microstructural-element body, viz. the B2 phase (α), the glassy phase (β), and phase consisting to equal parts of α and β ($\alpha\beta$). Physically, the $\alpha\beta$ -element can be regarded as effective interface between the α and the β phases. The fracture strain can then be described by

$$\varepsilon_f^c = f_{\alpha c} \varepsilon_f^\alpha + f_{\beta c} \varepsilon_f^\beta + \kappa f_{\alpha\beta} \varepsilon_f^{\alpha\beta}, \quad (3)$$

where $f_{\alpha c}$, $f_{\beta c}$, and $f_{\alpha\beta}$ are the corrected volume fraction of element α , β , and $\alpha+\beta$, ε_f^α , ε_f^β , and $\varepsilon_f^{\alpha\beta}$ are the fracture strain of α phase, β phase, and homogenous $\alpha+\beta$ composite, respectively, and κ is a dimensionless constant accounting for the constraint effect of the element α and/or element β on the element $\alpha+\beta$.¹⁵ Regardless of the value for $\kappa(\varepsilon_f^{\alpha\beta}/\varepsilon_f^\alpha)$ Eq. (3) is capable to capture the measured fracture strains. The best fit is obtained with $\kappa(\varepsilon_f^{\alpha\beta}/\varepsilon_f^\alpha) = 10$.

At stresses around 490 ± 30 MPa (Table I) the B2 phase yields and the fracture stress exceeds 2100 MPa. Such a pronounced hardening behavior is only known for transformation-induced plasticity materials. The deformation of the crystalline specimens was monitored *in situ* with high energy x rays to follow the evolution of martensite. Figure 3 shows a two-dimensional (2D) diffraction image of the undeformed (left half) and deformed sample at a stress of 1100 MPa (right half). The integrated 2D diffraction data are shown in the inset of Fig. 3. At a stress of 0 MPa the Bragg reflections correspond to B2 CuZr next to some weak reflections of $\text{Cu}_{10}\text{Zr}_7$. Apparently, partial decomposition into the low temperature equilibrium phases cannot be fully avoided

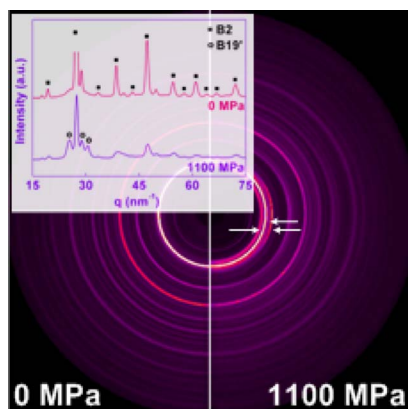


FIG. 3. (Color online) 2D diffraction image of the fully crystalline $\text{Cu}_{47.5}\text{Zr}_{47.5}\text{Al}_5$ sample unstressed (left half) and at 1100 MPa. The arrows show the strongest peaks of the new phase (B19'), which forms induced by plastic deformation. The inset shows the integrated 2D diffraction images in the undeformed (upper pattern) and deformed (lower pattern) states. Note that the strongest reflection of B2 CuZr has been cut off in the upper diffraction pattern.

during the thermal cycling. At a stress of 1100 MPa new Bragg peaks can be detected, which are allocated to B19' CuZr (martensite). Obviously, the work hardening of the B2 phase must be attributed to the martensitic transformation from B2 CuZr to B19' in the fully crystalline sample. Remarkably, even for low volume fractions the work hardening of the B2 crystals leaves its fingerprints in the stress-strain curves of the composite material.

It is known that a change in the matrix composition due to the precipitation of crystals leads to hardening.¹⁶ In the investigated CuZr-based alloys, however, B2 CuZr crystallizes polymorphically. Energy-dispersive x-ray spectroscopy proves that the crystals and the glassy matrix are of the same composition. Consequently, this mechanism cannot apply. The elastic properties of the glassy and the B2 phase were furthermore analyzed by ultrasonic measurements. Surprisingly, all three, Young's, shear, and bulk modulus of the glassy and the crystalline B2 phase are nearly identical (Table I). Although being structurally completely different, the glassy and crystalline phases are highly compatible. Hofmann *et al.*¹⁷ recently reported a similar compatibility of the crystalline and glassy phase in a β -Zr(Ti) reinforced alloy. They concluded that next to the appropriate length scale of the reinforcing phase the fundamental elastic properties of matrix and second phase have to match to enhance the toughness of the material. We believe that the good match of the shear moduli facilitates the slip transfer from the matrix to the B2 crystals. The glassy matrix deforms by shear banding and the shear is imposed on the crystalline phase when a shear band reaches the interface with a crystal. The propagation of shear band will be inhibited by the deformation and work hardenability of the B2 phase, which results in the nucleation of more shear bands.

Work hardening also occurs in a $\text{Cu}_{47.5}\text{Zr}_{47.5}\text{Al}_5$ BMG composite containing nanocrystals or structural heterogeneities on the nanometer scale (clusters).^{18–20} However, there are hints that the deformation and hardening processes in the nanocrystals are distinct from the ones in BMG composites containing micrometer-scale crystals. When the grain size is reduced to only a few nanometers in pure Cu (Ref. 21) and

pure Al (Ref. 22) deformation and hardening is mediated through twinning. Similarly, NiTi nanocrystals embedded in an amorphous matrix show fine compound twinning due to the high residual stresses in the composite.²³ Thus, when the grain size of “martensitic” BMG matrix composites is reduced to the nanometer scale the shear transformation and with it the work hardening is supposed to be borne by twinning.

To conclude, the polymorphic precipitation of B2 CuZr significantly enhances the fracture strain and decreases the yield strength under compressive loading. For this effect the observed high compatibility of the elastic moduli of the crystalline and glassy phase is essential. The work hardening found in the composites with micrometer-sized crystals can be ascribed to the strain-induced martensitic transformation inherent in CuZr-based alloys. The intrinsic hardenability of the crystals is also seen in the composites. This leads to the desired combination of high yield strength inherited from the glassy matrix and considerable plastic strain next to work hardening. Therefore, combining the shape memory effect and BMGs represents a fundamental route to synthesize a new class of composite materials with enhanced mechanical properties.

The EU research and training network on Ductile BMG Composites (MRTN-CT-2003-504692), the Global Research Laboratory Program of the Korean Ministry of Education, Science and Technology, and the Promotionsförderung des Cusanuswerks are acknowledged.

¹E. Pekarskaya, C. P. Kim, and W. L. Johnson, *J. Mater. Res.* **16**, 2513 (2001).

²J. Eckert, J. Das, S. Pauly, and C. Duhamel, *J. Mater. Res.* **22**, 285 (2007).

³H. Li, G. Subhash, L. J. Kecskes, and R. J. Dowding, *Mater. Sci. Eng., A* **403**, 134 (2005).

⁴Y. C. Kim, E. Fleury, J. C. Lee, and D. H. Kim, *J. Mater. Res.* **20**, 2474 (2005).

⁵A. Inoue, *Acta Mater.* **48**, 279 (2000).

⁶A. Inoue and W. Zhang, *Mater. Trans.* **43**, 2921 (2002).

⁷Y. N. Koval, G. S. Firstov, and A. V. Kotko, *Scr. Metall. Mater.* **27**, 1611 (1992).

⁸D. Schryvers, G. S. Firstov, J. W. Seo, J. Van Humbeeck, and Y. N. Koval, *Scr. Mater.* **36**, 1119 (1997).

⁹K. Otsuka and X. B. Ren, *Intermetallics* **7**, 511 (1999).

¹⁰K. J. Zeng, M. Härmäläinen, and H. L. Lukas, *J. Phase Equilib.* **15**, 577 (1994).

¹¹S. Pauly, J. Das, J. Bednarcik, N. Mattern, K. B. Kim, D. H. Kim, and J. Eckert, *Scr. Mater.* **60**, 431 (2009).

¹²V. C. Nardone and K. M. Prew, *Scr. Metall.* **20**, 43 (1986).

¹³D. Stauffer and A. Aharony, *Introduction to Percolation Theory* (Taylor and Francis, London, 1992).

¹⁴Z. Fan and A. P. Miodownik, *Scr. Metall. Mater.* **28**, 895 (1993).

¹⁵G. Liu, J. Sun, C. W. Nan, and K. H. Chen, *Acta Mater.* **53**, 3459 (2005).

¹⁶A. L. Greer, *Mater. Sci. Eng., A* **304**, 68 (2001).

¹⁷D. C. Hofmann, J. Y. Suh, A. Wiest, G. Duan, M. L. Lind, M. D. Demetriou, and W. L. Johnson, *Nature (London)* **451**, 1085 (2008).

¹⁸J. Das, M. B. Tang, K. B. Kim, R. Theissmann, F. Baier, W. H. Wang, and J. Eckert, *Phys. Rev. Lett.* **94**, 205501 (2005).

¹⁹K. B. Kim, J. Das, F. Baier, M. B. Tang, and W. H. Wang, *Appl. Phys. Lett.* **88**, 051911 (2006).

²⁰K. B. Kim, J. Das, M. H. Lee, S. Yi, E. Fleury, Z. F. Zhang, W. H. Wang, and J. Eckert, *J. Mater. Res.* **23**, 6 (2008).

²¹L. Lu, X. Chen, X. Huang, and K. Lu, *Science* **323**, 607 (2009).

²²M. W. Chen, E. Ma, K. J. Hemker, H. W. Sheng, Y. M. Wang, and X. M. Cheng, *Science* **300**, 1275 (2003).

²³T. Waitz and H. P. Karnthaler, *Acta Mater.* **52**, 5461 (2004).